Categorization of the Glaciated Terrain of Indian Himalaya using CP and FP mode SAR

Gulab Singh, *Member, IEEE*, Yoshio Yamaguchi, *Fellow, IEEE*, Sang-Eun Park, *Member, IEEE*, Wolfgang-Martin Boerner, *Life Fellow, IEEE*, Yi Cui, *Member, IEEE,* Gopalan Venkataraman, *Member, IEEE*

***Abstract*—This paper presents the comparison between the potential of synthetic aperture radar (SAR) data in compact polarimetry (CP) *versus* the fully polarimetric POLSAR mode (FP) for glacier areas. The eigenvalue-based constructed parameters, decompositions and supervised classification schemes were used for this inter-comparison. The comparison is focused on compact polarimetric techniques *versus* full polarimetric techniques based on both of qualitative and quantitative analysis of the glaciated parameters extraction. Overall performance of CP mode is lower than FP mode for glaciated terrain parameter extraction. Furthermore, it was found over the part of rugged Gangotri glaciated terrain, Indian Himalaya that the reconstruction pseudo polarimetry data is erroneous and highly biased because of data sets do not satisfy the pseudo polarimetric reconstruction conditions in the glaciated terrain.**

***Index Terms*—Remote sensing, mono polarimetry (MP), dual polarimetry (DP), compact polarimetry (CP), full polarimetry (FP), SAR, snow, Himalaya, Glacier, Gangotri.**

I. INTRODUCTION

At present two lunar orbital missions such as Chandrayaan-1 and Lunar reconnaissance orbiters with their respective sensor MiniSAR (miniature synthetic aperture radar) and MiniRF (miniature radio frequency) and the Indian RISAT-1 (radar imaging satellite -1) are acquiring data in the hybrid polarity mode (CP) [1], [2]. But in recent days, the implementation of fully polarimetric radar *versus* compact polarimetric radar systems for land observation has become a topical debate for assessing which one is more advantageous. Nowadays, the interest of researchers and space agencies in compact polarimetry is growing quickly. Since land parameters play important roles in environmental assessments, several studies [3] - [7] were done for evaluating the capability of compact polarimetry to monitor various land parameters such as vegetation/forest [3], [4], man-made structure [5], soil moisture [6] and etc.. Some of the forthcoming sensor systems such as SAOCOM 1A (satélite Argentino de observación con microondas 1A) of the Argentine Space Agency, ALOS-2 (advanced land observation satellite -2) of the Japan Aerospace Exploration Agency JAXA, the Canadian RADARSAT constellation mission (RCM), and the American DESDynl (deformation, ecosystem structure and dynamics of ice) in very near-future may be operating in so called compact polarimetry (CP) mode next to the proven full polarimetric mode (FP) for land observations [7]. Out of several land parameters, the glaciated terrain parameters (snow-cover/snow-line, glacier ice, etc.) play a crucial role for predicting, and modeling climate change, flood, local weather, avalanche forecast and economical optimization for the hydropower production in high mountainous areas as well as agricultural irrigation procedures. However, these applications need timely information about glaciated terrain parameters and their temporal and spatial variability for which field measurements are difficult to conduct regularly and may not be representative of the spatial variability. Since snow-cover/snow-line consists of strong spatial and time- dependent parameters, frequent observation cycles are necessary. Optical remote sensing provides promising results under optimal meteorological conditions, but it fails under cloud and adverse weather conditions. Radar remote sensing has an advantage over visible and near infrared techniques due to its all weather capability, penetration through clouds and its quasi independence of sun illumination. Recently, through extensive field exploration and analysis, it was concluded by Singh and Venkataraman [8] that synthetic aperture radar data with quad polarization mode (FP) measurements have produced most encouraging results for discrimination of snow from other associated scatterers and mapping of snow cover extent as compared to conventional SAR data with single mono polarization (MP) and dual polarization (DP) mode measurements.

It is now necessary to explore the potential of fully polarimetric (FP) *versus* hybrid compact polarimetric (CP) modes for snow/ice feature detection on the earth as well as on planetary surfaces. Hence, this paper contributes to the ongoing discussion answering the following question: is there a distinct advantage and necessity of SAR acquisition in quad polarization (FP) as compared to SAR acquisitions in compact-hybrid polarization (CP) over the rugged glaciated terrain (Himalayas)?

II. STUDY AREA

This study was performed over the Gangotri Glacier, which lies in the north-west part of the Indian Himalayan snow and glacier covered region (Fig.1). The altitude of the Gangotri Glacier ranges from 4000 to 7000 m. The length of the Gangotri Glacier is about 30 km width varies from 0.5 to 2.5 km. The Gangotri Glacier is the second longest glacier in the entire

Manuscript received August 28, 2012; revised April 25, 2013 and May 14, 2013; accepted May 30, 2013.

G. Singh, Y. Yamaguchi, S.-E. Park and Y. Cui are with Graduate School of Science and Technology, Niigata University, Japan.

W.-M. Boerner is with the University of Illinois at Chicago, United state of America.

G. Venkataraman is with the Centre of Studies in Resources Engineering, Indian Institute of Technology Bombay, Mumbai, India.

Indian Himalayan ranges. Numerous small sized glaciers also join the main Gangotri glacier from all sides and form the Gangotri group of glaciers. The main glacier as well as its tributaries are valley glaciers. The total ice cover is approximately 300km^2 and has about 20 km^3 of ice in volume. The main Gangotri glacier drains in the northwesterly direction from the peaks. The Bhagirathi River originates at the snout of the glacier located at Gaumukh in the northern most end of the glacier. The center of the blue color line star illustrates the snout position in Fig. 1. Sub glacial channels also feed the Bhagirathi River at Gaumukh.

Radar imagery of ALOS-PALSAR over the Gangotri Glacier and near-real time field information provide an ideal test site for applying full polarimetry *versus* compact polarimetry for the comparison of the potential of the categorization of glaciated terrain in Indian Himalayan regions.

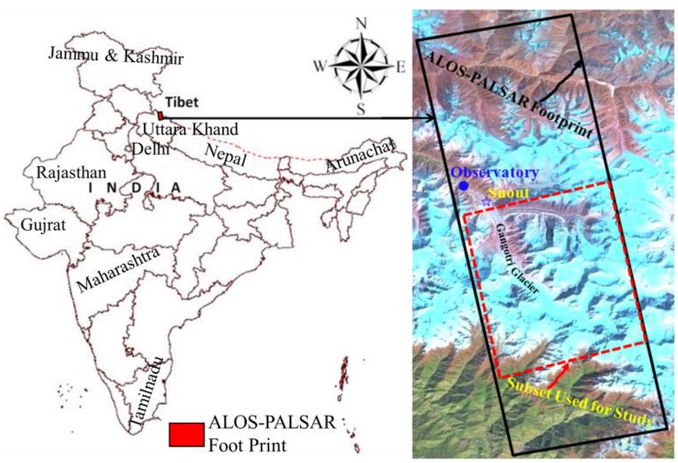

Fig. 1. Location of the test site within the Indian Himalayan region, The Gangotri Glacier is shown in left image with the location of the SASE's observatory (blue circle) and snout of the glacier (center of the blue color line star) at Gomukh. The black line box denotes the ALOS-PALSAR image footprint and red dashed line box represents the used subset area of images for the analysis under this study.

III. Material and Methods

A. Field Data

The observatory of the Snow and Avalanche Establishment, Manali, India collected field data on the Gangotri glaciated terrain. The field station data are provided in Table I. Location of field data is marked in Fig.1 with blue circle.

Table I. Bhojbasa Field station data

Altitude (m)	Date	Sunshine Duration (h/day)	Max. Temp. (^{0}C)	Min. Temp. (^{0}C)	Standing Snow (cm)
3800	24-05-2010	9.5	19.5	1.5	0
3800	06-06-2010	7.5	17	0	0

B. SAR Polarimetry Data Availability

Although C-band (5.35 GHz) compact hybrid polarimetry RISAT-1 mission is operating for earth observation but a non-availability of compact hybrid polarimetry data with us, L-band (1.27GHz) fully polarimetric ALOS-PALSAR single look complex, level 1.1 data were converted into compact hybrid polarimetry and the pseudo coherency matrix was reconstructed based on existing matrix formulations for further examination. ALOS-PALSAR acquired fully polarimetric data sets over the Gangotri Glacier on June 06, 2010 with 23.1^0 off-nadir angle in ascending orbit at local time 22:37 hrs. Furthermore, the cloud free images of advanced visible near infrared radiometer-2 (AVNIR-2) are used to interpret the behavior of the glacier area although acquired at a different day (May 24, 2010 and local time 11:02 AM), AVNIR-2 was one of the three sensors of the Advanced Land Observation Satellite (ALOS).

1) Covariance Matrix: The acquired backscattering matrix $\boldsymbol{S}$ for fully polarimetric SAR (Full-POLSAR) can be defined by the three- dimensional backscattering vector $\boldsymbol{k_L}$ as:

$$\boldsymbol{k_L} = \left[S_{HH} \quad \sqrt{2}S_{HV} \quad S_{VV}\right]^T \tag{1}$$

where the element of backscattering matrix S_{HH}, S_{VV}, S_{HV} are called complex backscattering coefficients. Superscript ^{T} denotes transpose of matrix.

The 3x3 polarimetric covariance matrix $\langle[\boldsymbol{C}]\rangle$ for the reciprocal case can be defined as

$$\langle[\boldsymbol{C}]\rangle = \langle \boldsymbol{k_L}\boldsymbol{k_L}^{*T}\rangle = \begin{bmatrix} \langle|S_{HH}|^2\rangle & \sqrt{2}\langle S_{HH}S_{HV}^*\rangle & \langle S_{HH}S_{VV}^*\rangle \\ \sqrt{2}\langle S_{HV}S_{HH}^*\rangle & 2\langle|S_{HV}|^2\rangle & \sqrt{2}\langle S_{HV}S_{VV}^*\rangle \\ \langle S_{VV}S_{HH}^*\rangle & \sqrt{2}\langle S_{VV}S_{HV}^*\rangle & \langle|S_{VV}|^2\rangle \end{bmatrix} \tag{2}$$

where $*^T$ denotes complex conjugation and transposition, and ‹•› denotes ensemble average in an imaging window.

2) Pseudo-Covariance Matrix: If the SAR transmits left circular polarization and receives in the *HV* polarization basis, then compact polarimetry scattering vectors can be written as

$$\boldsymbol{k_{CP(L)}} = \frac{1}{\sqrt{2}}[S_{HH} + j\,S_{HV} \quad jS_{VV} + S_{HV}]^T \tag{3}$$

The factor √2 in (3) implies a 3-dB loss in the radar signal with respect to conventional dual or full polarimetric modes. This is an inevitable consequence of mismatching the transmitter and receiver polarimetric basis [3], [9].

$$\langle[\boldsymbol{C_2}]\rangle = \langle \boldsymbol{k_{CP(L)}}\boldsymbol{k_{CP(L)}^{*T}}\rangle = \begin{bmatrix} \langle \boldsymbol{J_{11}}\rangle & \langle \boldsymbol{J_{12}}\rangle \\ \langle \boldsymbol{J_{21}}\rangle & \langle \boldsymbol{J_{22}}\rangle \end{bmatrix} \tag{4}$$

$$\begin{aligned} \langle \boldsymbol{J_{11}}\rangle &= 0.5(\langle S_{HH}^2\rangle + \langle S_{HV}^2\rangle + 2\,Im\{\langle S_{HH}S_{HV}^*\rangle\}) \\ \langle \boldsymbol{J_{12}}\rangle &= 0.5(\langle S_{HH}S_{HV}^*\rangle - j\langle S_{HH}S_{VV}^*\rangle + \langle S_{HV}S_{VV}^*\rangle + j\langle S_{HV}^2\rangle) \\ \langle \boldsymbol{J_{21}}\rangle &= \langle J_{12}^*\rangle \\ \langle \boldsymbol{J_{22}}\rangle &= 0.5(\langle S_{VV}^2\rangle + \langle S_{HV}^2\rangle + 2\,Im\{\langle S_{HV}S_{VV}^*\rangle\}) \end{aligned} \tag{5}$$

Equation (5) includes 9 unknowns and 4 compact-pol covariance observations: to invert the linear system additional relationships are required. Since compact polarimetric scattering models assume that polarimetric scattering is reflection symmetric, and thus the co-pol/cross-pol correlations are set to zero. This simplification often applies reasonably well for analysis of natural scatterers at various frequencies [10] as long as heterogeneous volume scattering is neglected [11]-[15]. Under the assumption of reflection symmetry the quad-pol covariance matrix becomes a function of five independent variables. Under the reflection symmetry condition, (5) becomes (6) respectively, which is defined as

$$
\begin{aligned}
\langle \boldsymbol{J_{11}} \rangle &= 0.5(\langle S_{HH}^2 \rangle + \langle S_{HV}^2 \rangle \}) \\
\langle \boldsymbol{J_{12}} \rangle &= 0.5(-j\langle S_{HH} S_{VV}^* \rangle + j\langle S_{HV}^2 \rangle) \\
\langle \boldsymbol{J_{21}} \rangle &= \langle \boldsymbol{J}_{12}^* \rangle \\
\langle \boldsymbol{J_{22}} \rangle &= 0.5(\langle S_{VV}^2 \rangle + \langle S_{HV}^2 \rangle \})
\end{aligned} \tag{6}
$$

Still (6) has only five unknowns with four known independent variables, and so one cannot solve for all five elements of $\langle [\boldsymbol{C}] \rangle$ under reflection symmetry condition [9]. Therefore, an additional constraint equation between the elements of $\langle [\boldsymbol{C}] \rangle$ under the reflection symmetry condition is required to reduce the number of unknown to four for constructing the reflection-symmetric pseudo-quad-pol data covariance matrix $\langle [\boldsymbol{C_{CP}}] \rangle$ from compact polarimetric imagery [3]. Souyris *et al.* [4] defined a non-linear relationship between the elements of $\langle [\boldsymbol{C}] \rangle$ under the reflection symmetry condition. By using (6) with the non-linear relation of Souyris *et al.* [4] to yield the cross-polarized terms under the reflection symmetry combined with the additional constraints of rotation invariance, the elements of (7) $\langle [\boldsymbol{C_{CP}}] \rangle$ can be solved by iteration [16]. The pseudo polarimetric covariance matrix under rotation and reflection symmetries for left circular transmit and orthogonal *H-V* receive, can be written as [3]

$$
\langle [\boldsymbol{C_{CP}}] \rangle = \frac{1}{4} \begin{bmatrix} \langle C_{11}^{CP} \rangle & 0 & \langle C_{13}^{CP} \rangle \\ 0 & \langle C_{22}^{CP} \rangle & 0 \\ \langle C_{31}^{CP} \rangle & 0 & \langle C_{33}^{CP} \rangle \end{bmatrix} \tag{7}
$$

Despite the system and theoretical justification issues, this form of the CP-restricted PolSAR covariance matrix has been used to examine compact SAR applications for glaciated terrain parameters information and compare the information contents of full polarimetry with that of compact polarimetry, as will be discussed in the next section. However, (7) is the shifting of (4), using a 2x2 to 3x3 process and that literature emphasizes an unavoidable loss of information in regard of FP mode but the conditions for reconstruction of the pseudo polarimetric data are not satisfied in the glaciated region and reconstruction of data will highly biased (see Section IV for the results).

C. Entropy and Alpha

Based on this eigenvalue decomposition [17] the secondary parameters such as entropy and alpha can be defined as function of the eigenvalues of the coherency matrix. The degree of randomness of each target or the degree of statistical disorder of each target is known as the entropy. The entropy (H) can be defined using the definition of *von Neumann* as the logarithmic sum of the eigenvalues of covariance or coherency matrix as

$$
H = -P_1 log_3 P_1 - P_2 log_3 P_2 - P_3 log_3 P_3 \tag{8}
$$

$$
0 \le P_i = \frac{\lambda_i}{\sum_{i=1}^{3} \lambda_i} \le 1 \tag{9}
$$

where P_i are pseudo-probabilities, which can be obtained from the eigenvalues λ_i.

The mean scattering ($\bar{\alpha}$) angle varies from 0^0 to 90^0.

$$
\bar{\alpha} = P_1\alpha_1 + P_2\alpha_2 + P_3\alpha_3 \tag{10}
$$

Total power (TP) is defined as

$$
TP = \lambda_1 + \lambda_2 + \lambda_3 \tag{11}
$$

D. Polarization Fraction

The polarization fraction (PF) is defined [18] as

$$
PF = 1 - \frac{3\lambda_3}{TP};\ 0 \le PF \le 1 \tag{12}
$$

*E. **m**-χ Decomposition*

An alternative decomposition methodology for compact polarimetric radar data, based on 2 x 2 covariance matrix data product often in the form of the four Stokes parameters ($\mathbf{S_0}$, $\mathbf{S_1}$, $\mathbf{S_2}$, and $\mathbf{S_3}$) was introduced for the MiniSAR concept by Raney [1], [2]. One example of CP decomposition approaches [7], [19], [20] is an $\boldsymbol{m}$-χ decomposition [19] for which $\boldsymbol{m}$ is the degree of polarization of the observed field and χ is the Poincaré ellipticity parameter.

$$
\mathbf{S_0} = \langle \mathbf{J_{11}} \rangle + \langle \mathbf{J_{22}} \rangle \tag{13}
$$

$$
\mathbf{S_1} = \langle \mathbf{J_{11}} \rangle - \langle \mathbf{J_{22}} \rangle \tag{14}
$$

$$
\mathbf{S_2} = \mathbf{2Re} \langle \mathbf{J_{12}} \rangle \tag{15}
$$

$$
\mathbf{S_3} = -\mathbf{2Im} \langle \mathbf{J_{12}} \rangle \tag{16}
$$

$$
\boldsymbol{m} = \frac{\sqrt{(\boldsymbol{S_1^2} + \boldsymbol{S_2^2} + \boldsymbol{S_3^2})}}{\boldsymbol{S_0}} \tag{17}
$$

$$
\sin 2\chi = -\frac{\mathbf{S_3}}{\mathbf{S_0}\boldsymbol{m}} \tag{18}
$$

Equation (18) also represents the degree of circularity.

The $\boldsymbol{m}$-χ decomposition scheme has been used for generating the RGB image. For producing the RGB image, the first Stokes parameter ($\mathbf{S_0}$), $\boldsymbol{m}$ and χ are included in this decomposition scheme as [19]

$$
\begin{bmatrix} P_d \\ P_v \\ P_s \end{bmatrix} = \begin{bmatrix} \sqrt{\mathbf{S_0}\boldsymbol{m}(\frac{1+\sin 2\chi}{2})} \\ \sqrt{\mathbf{S_0}(1-\boldsymbol{m})} \\ \sqrt{\mathbf{S_0}\boldsymbol{m}(\frac{1-\sin 2\chi}{2})} \end{bmatrix} \tag{19}
$$

The parameters $\mathbf{S_0}$, $\boldsymbol{m}$, and χ, in the right hand side of (19) are independent to an orientation angle [9].

F. Full-POLSAR model based decomposition: G4U

General 4-component scattering power decomposition with unitary transformation (G4U) of the coherency matrix has been implemented on fully polarimetric SAR data. Transformation $\langle[\boldsymbol{C}]\rangle$ to the coherency matrix $\langle[\boldsymbol{T}]\rangle$ is made before implementation because double unitary transformations of $\langle[\boldsymbol{T}]\rangle$, as proposed in [21], are easy and simple.

$$[U(\varphi)][T(\theta)][U(\varphi)]^{\dagger}$$
$$= [U(\varphi)](f_s[T]_s + f_d[T]_d + f_v[T]_v + f_c[T]_c)[U(\varphi)]^{\dagger} \quad (1)$$

where † denotes complex conjugation and transposition, and the unitary transformation matrix $U(\varphi)$ and φ are introduced in [21]; $[T(\theta)]$ denotes the measured coherency after orientation compensation [22]; f_s, f_d, f_v and f_c are coefficients to be determined; $[T]_s$, $[T]_d$, $[T]_v$ and $[T]_c$ are expansion matrices corresponding to the surface, double bounce, volume, and helix scattering, respectively [22]. G4U accounts all polarimetric parameters with extended volume scattering and produces promising results. Results of G4U are used for comparing the results of $\boldsymbol{m}$-χ decomposition.

IV. Results

A. Compact versus Fully Polarimetric Decomposition Results

The potential of the compact polarimetry SAR data has been explored based on the $\boldsymbol{m}$-χ decomposition approach [18], which is performed better than earlier the $\boldsymbol{m}$-$\boldsymbol{\delta}$ approach [2], [7]. These approaches are dedicated to compact polarimetric SAR data decomposition for obtaining the results similar to results of fully polarimetric scattering power decomposition scheme [7], [20]. Fig. 2 shows visually the inter-comparison of G4U RGB (Red-Green-Blue) and the $\boldsymbol{m}$-χ RGB approach. In these RGBs, Red indicates double-bounce scattering, Green corresponds to the volume scattering and Blue represents the surface scattering. However, all RGB images are made with common color scale for which the $\boldsymbol{m}$-χ RGB images look different from fully polarimetric RGB images. Green contribution is low in the $\boldsymbol{m}$-χ RGB image compared to G4U RGB image.

As can be found, the $\boldsymbol{m}$-χ RGB images provide snow-line detection capabilities which are similar to that of fully polarimetric RGB. In addition, the ablation area of the glacier is highly crevassed and covered with moraine and debris materials (see field photo in Fig. 2) which represents the random scattering area. This area appears green in the decomposition RGB images. The snowpack is wet during the melting phase in June. It can be seen from Table I and AVNIR-2 image in Fig. 2 that it was warmer temperature (with good sunshine) and approximately half of the seasonal snowpack cover has been melting from the main glacier body during the day of ALOS-PALSAR observation. Wet snowpack is represented in blue color in the decomposition image because the surface scattering is dominant.

B. Pseudo versus True full Polarimetric Parameters

In this investigation, based on the eigenvalues of (2) [true full polarimetric covariance matrix (TFPCM)] and (7) [pseudo-polarimetric covariance matrix (P_2CM)] other parameters such as entropy (H), scattering mechanism angle (α) and polarization fraction (PF) have been analyzed. Polarimetric parameters H, $\bar{\alpha}$, P_1, P_2, P_3, and PF of TFPCM and P_2CM are applied to the PALSAR image acquisition over the Gangotri Glacier, being a part of the North–West Indian Himalayan glaciated region. P_2, P_3, H and $\bar{\alpha}$, provide lower values over the snow cover and a higher value over the other distributed/random scatterers (e.g. ablation area of debris covered glacier, natural dihedral targets). However, P_1 and PF exhibit a higher value over snow area and lower value over the other areas. Due to surface scattering dominance over snow covered areas, the scattering mechanism angle ($\bar{\alpha}$) represents low value over snow covered areas. However, eigenvalues of P_2CM based derived H, $\bar{\alpha}$, and TP parameters give similar patterns as compared to H, $\bar{\alpha}$, and TP parameters of TFPCM [23]. Singh *et al.* [23] clearly demonstrated that the comparisons in between the P_1, P_2, P_3, H, $\bar{\alpha}$ and PF with and without reflection symmetry condition are not one to one correlated for snow cover but these parameters were still toughly akin over the Himalayan snow covered glaciated terrain. Ainsworth *et al.*, [5] have shown in their study that the derived P_2CM does not provide results relative to the results of TFPCM in the urban areas but with the construction of the P_2CM does permit a direct comparison of the derived polarimetric parameters for the FP *versus* CP modes. Here, a comparison by statistical procedures has been carried out between several parameters P_1, P_2, P_3, H, $\bar{\alpha}$, PF, of P_2CM *versus* TFPCM. The scatter plots of P_1, P_2, P_3, H, $\bar{\alpha}$, PF, for P_2CM *versus* TFPCM for yellow-dashed-lines profiles on G4U RGB in Fig. 2 are shown in Figs. 3(a), 3(b), 3(c), 3(d), 3(e) and 3(f) respectively. The correlation between results of TFPCM *versus* P_2CM is not strong and with biases being also high.

These results indicate that the pseudo polarimetric reconstruction conditions in rugged Indian Himalayan glaciated terrain are not applicable for expanding the compact polarimetric 2x2 covariance matrix to the conventional 3x3 covariance matrix. This cause will decrease the estimation performance of the polarimetric parameters; finally this problem will translate into the estimation performance of the glaciated terrain parameters [23]. So, applying Full-POLSAR techniques on reconstructed pseudo polarimetric information is not a good idea for categorizing the glaciated terrain parameters.

C. Compact versus Fully Polarimetric data: Supervised Classification Results

Since reconstructions of fully polarimetric parameters are erroneous, the supervised Wishart classification technique [5], [18], [24] was implemented for the fully polarimetric and compact polarimetric covariance matrices directly; and training sets for the snow-cover class and other classes have been allotted on the basis of visually comparing decomposition color combination image with AVNIR-2 snow-cover image. Based on the same training sets, CP and FP SAR data have been classified into five major classes including snow-cover, transition zone (TZ), debris covered glacier (DCG), vegetation/rock and others (Fig. 4). Overall accuracies of fully polarimetric and compact polarimetric data sets based classification are 90.29% and 86.12% respectively (see Table II and Table III). It is clear from the Tables II and III that fully polarimetric data sets produce 4% higher overall accuracy as compared to compact polarimetric data sets. However, the user accuracies for the snow and transition zone TZ classes in the fully polarimetric SAR data are 7.19% and 7.26% higher than the compact polarimetric SAR data. Producer's accuracy of the TZ class in both polarimetric data classifications also indicates that the discrimination capability of the TZ area in the CP supervised classification scheme is remarkable low. Both user's and producer's accuracies of the compact polarimetric classification scheme in the DCG class are found to be very close to the fully polarimetric classification scheme.

Finally, a McNemar test [25], [26] was performed to compare the classification results of CP with the results of FP and the obtained McNemar's value 14.8662 is greater than the critical value 3.8415 with one degree of freedom at 5 % significance level. This indicates that the performance of between two classification results (CP *versus* FP) is different.

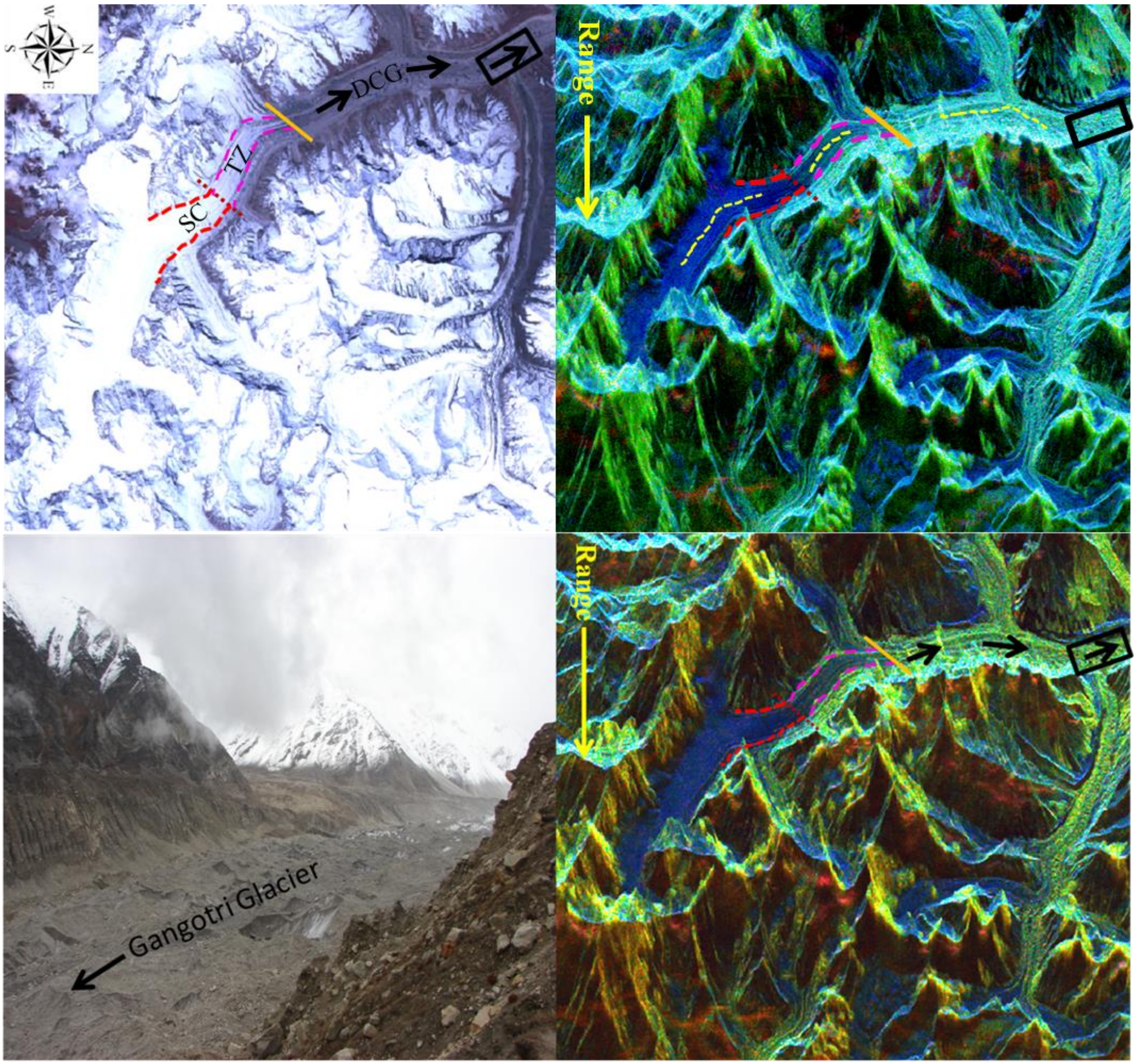

Fig.2. **Top row:** (left) ALOS-AVNIR-2 RGB image of 24-05-2010 over Gangotri glacier and (right) G4U RGB of ALOS-PALSAR with 12 × 2 multi-look (azimuth × range) factors of 06-06-2010 over Gangotri glacier [Red: double bounce scattering, Green: volume scattering, Blue: surface scattering]; **Bottom Row:** (left) a field photo (18-09-2006) of the black rectangular area and (right) $\boldsymbol{m}$- $\boldsymbol{\chi}$ RGB of ALOS-PALSAR with 12 × 2 multi-look (azimuth × range) factors of 06-06-2010 over Gangotri glacier [Red: double bounce scattering, Green: volume scattering, Blue: surface scattering];. The magenta dashed lines cover the transition zone [transition zone represents the shifting from the snow laden zone on debris covered glacier areas to the debris covered glacier areas, due to the melting of snow] in between wet snow accumulated area above the red line (across the glacier) and the ablation area below the golden line. Note that the illustrations of ALOS images in this figure are rotated 90^0 clockwise from the original illustrations. Black line arrows represent the flow direction of glacier ice. The yellow dashed lines along the glacier in G4U RGB show the profile lines for scatter plots in Fig. 3 of snow-cover (SC), transition zone (TZ), and debris covered glacier (DCG) areas .

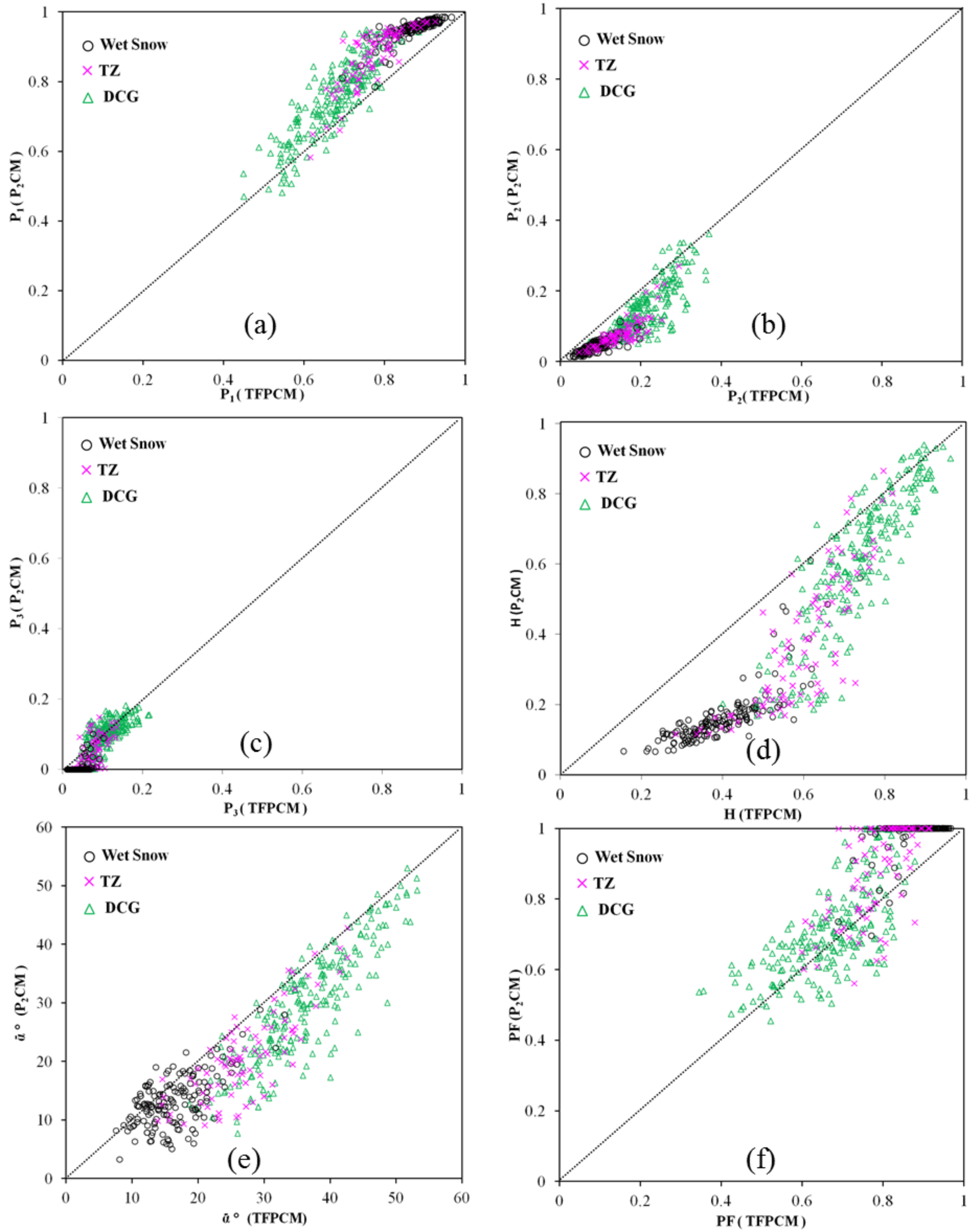

Fig. 3. Scatter plots of wet snow, transition zone (TZ) and debris covered glacier (DCG) areas for: (a) the probability of first eigenvalue (P_1) of TFPCM *versus* probability of P_2CM; (b) the probability of second eigenvalue (P_2) of TFPCM *versus* probability of P_2CM ; (c) the probability of third eigenvalue (P_3) of TFPCM *versus* the probability of P_2CM; (d) the entropy (H) of TFPCM *versus* entropy of P_2CM ; (e) the $\bar{\alpha}$ of TFPCM *versus* $\bar{\alpha}$ of P_2CM ; (f) the PF of TFPCM *versus* PF of P_2CM.

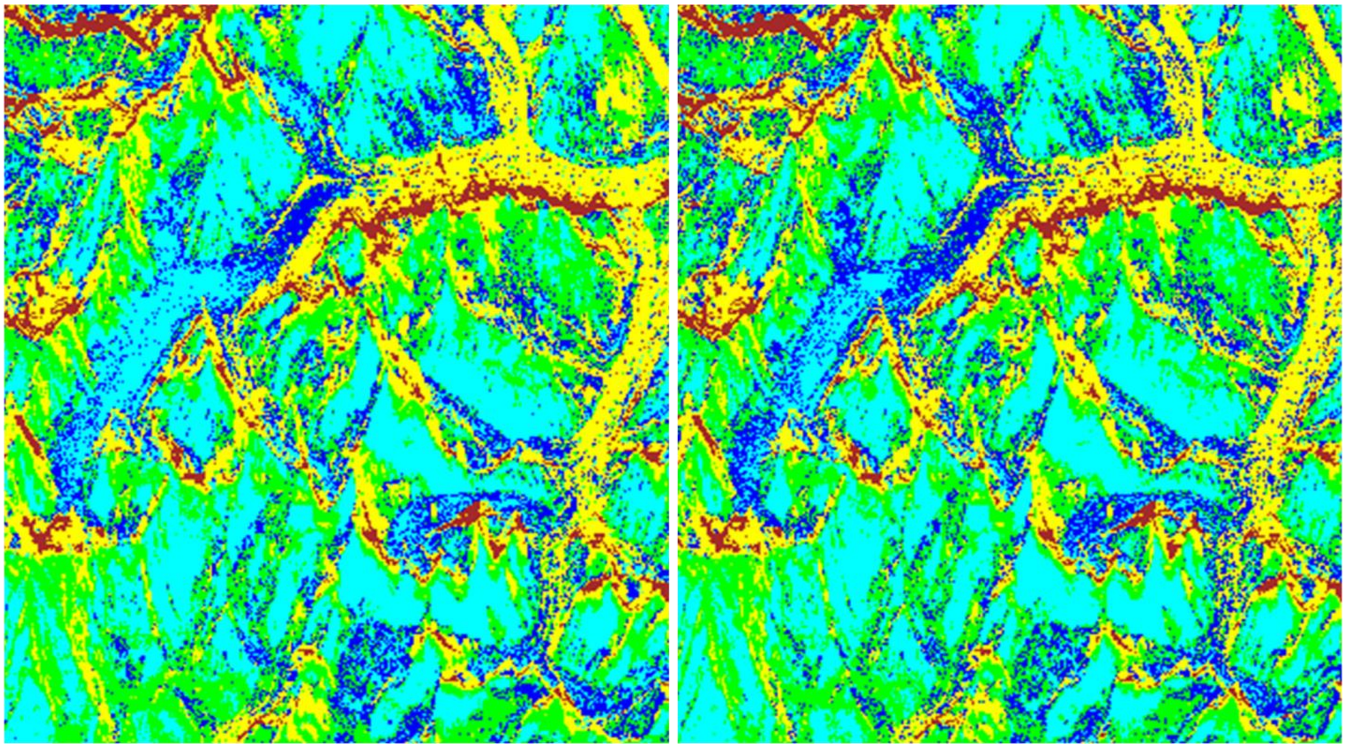

Fig.4. Wishart supervised classification maps: Fully polarimetric data based (left) and compact polarimetric data based (right). Note that the illustrations of ALOS images in this figure are rotated 90^0 clockwise from the original illustrations. In this figure, yellow color denotes DCG, blue color represents TZ, cyan color illustrates snow, green color indicates the vegetation/rock area and brown color demonstrates “Others” class (the unidentified or else layover areas due to steep slopes are taken as a special class “Others” in the Wishart supervised classification images).

TABLE II
CONFUSION MATRIX FOR FULLY POLARIMETRIC WISHART SUPERVISED CLASSIFICATION

	User Defined Sample					
Classified	Snow	TZ	DCG	Vegetation /Rock	Others	Row Sum
Snow	454	38	6	3	0	501
TZ	31	386	10	28	0	455
DCG	5	15	402	18	4	444
Vegetation/Rock	5	8	6	311	0	330
Others	0	0	23	0	308	331
Column Sum	495	447	447	360	312	2061
User’s Accuracy (%)	90.62	84.84	90.54	94.24	93.05	Overall accuracy = 90.29%
Producer’s Accuracy (%)	91.72	86.35	89.93	86.39	98.72	

TABLE III
CONFUSION MATRIX FOR COMPACT POLARIMETRIC WISHART SUPERVISED CLASSIFICATION

	User Defined Sample					
Classified	Snow	TZ	DCG	Vegetation /Rock	Others	Row Sum
Snow	418	64	8	11	0	501
TZ	48	353	12	42	0	455
DCG	7	23	393	17	4	444
Vegetation/Rock	6	14	4	306	0	330
Others	0	0	26	0	305	331
Column Sum	479	454	443	376	309	2061
User's Accuracy (%)	83.43	77.58	88.51	92.73	92.15	Overall accuracy = 86.12%
Producer's Accuracy (%)	87.26	77.75	88.71	81.38	98.71	

V. CONCLUSION

Both CP and FP mode SAR data are used to categorize the glaciated terrain over the Indian Himalayan region. Comparisons have been done between the compact and quad polarization, data sets for the potential of glaciated terrain characterization. After an extensive analysis and observations of present investigations, it is possible to conclude that fully polarimetric SAR techniques have produced promising results in all of the diverse scenario cases studied, and which is not the case for the CP techniques.

Moreover, results indicate that reconstruction based assessment may not useful for snow cover (accumulation zone) and transition zone, over the glaciated terrain. However, improved comparisons for simultaneously acquired L-Band versus S-Band, C-Band and X-Band CP and FP SAR image data would be essential for further clarification, which could be achieved with the implementation of the airborne multi-band DLR-HR F-SAR for which any three bands can be operated simultaneously.

ACKNOWLEDGMENT

The authors are grateful to JAXA for providing the desired fully polarimetric Quad-Pol ALOS-PALSAR data sets under RA project JAXA-555 and 599. The authors would like to thank Dr. Snehmani, Deputy Director, Snow and Avalanche Study Establishment, Chandigarh, India, for providing field condition.

REFERENCES

[1] R. K. Raney, "Hybrid-polarity SAR architecture", *IEEE Trans. Geosci. Remote Sens.*, vol 45, no. 11, pp. 3397-3404, 2007.

[2] R. K. Raney, "Dual polarized SAR and Stokes parameters," *IEEE Geosci. Remote Sens. Lett.*, vol. 3, no. 3, pp. 317–319, Jul. 2006.

[3] M. Lavalle, "Full and Compact Polarimetric Radar Interferometry for Vegetation Remote Sensing", Ph.D. Thesis, Université de Rennes 1, France, 2009.

[4] J. C. Souyris, P. Imbo, R. Fjortoft, S. Mingot, and J. S. Lee, "Compact polarimetry based on symmetry properties of geophysical media: The $\pi/4$ mode," *IEEE Trans. Geosci. Remote Sens.*, vol. 43, no. 3, pp. 634–646, Mar. 2005.

[5] T. L. Ainsworth, J. P. Kelly and J.-S. Lee, "Classification comparisons between dual-pol, compact polarimetric and quad-pol SAR imagery", *ISPRS Journal of Photogrammetry and Remote Sensing*, 64, pp. 464-471, 2009.

[6] M.L. Truong-Loi, A. Freeman, P. Dubois-Fernandez, and E. Pottier, "Estimation of Soil Moisture and Faraday Rotation From Bare Surfaces Using Compact Polarimetry," *IEEE Trans. Geosci. Remote Sens.*, vol. 47, no. 11, pp. 3608–3615, Nov. 2009.

[7] F.J. Charbonneau, B. Brisco, R.K. Raney, H. McNairn, C. Liu, P.W. Vachon, J. Shang, R. DeAbreu,C. Champagne, A. Merzouki, and T. Geldsetzer, " Compact Polarimetry overview and applications assessment", *Can. J. Remote Sens.*, vol. 36, no. S2, pp. S298-S315, 2010.

[8] G. Singh and G. Venkataraman, "Application of incoherent target decomposition theorems to classify snow cover over the Himalayan region," *Int. J. Remote Sens.*, vol. 33, no. 13, pp. 4161-4177, Jul. 2012.

[9] S. R. Cloude, *Polarisation: Applications in Remote Sensing*. London,U.K.: Oxford Univ. Press, 2009.

[10] A. Freeman and S.L Durden, "A three-component scattering model for polarimetric SAR data," *IEEE Trans. Geosci. Remote Sens.*, vol. 36, no. 3, pp. 936–973, May 1998.

[11] L. Tsang and Z. Chen, " Polarimetric passive and active remote sensing: theoretical modeling of random discrete scatterers and rough surfaces," In: *Proceeding of IEEE- Geoscience and Remote Sensing Symposium, 1990. IGARSS '90. 'Remote Sensing Science for the Nineties'., 10th Annual International*, pp.2201 – 2203, 1990.

[12] Z. Chen and L. Tsang, "Polarimetric signatures of a layer of nonspherical discrete scatterers overlying a homogeneous half-space based on full multiple scattering vector radiative transfer theory," *Microwave and Optical Technology Letters*, vol. 5, no.10, pp. 520-524, September 1992.

[13] L. Tsang, "Dense media radiative transfer theory for dense discrete random media with spherical particles of multiple sizes and permittivities," *Progress in Electromagnetics Research*, vol. 6, Dielectric Properties of Heterogeneous Materials, Chapter 5, 181-230, ed. by A. Priou, Elsevier, New York, 1992.

[14] L. Tsang, J. A. Kong, and R. Shin, *Theory of Microwave Remote Sensing*, Wiley-Interscience, New York, 1985

[15] L. Tsang, J.A. Kong, and K.H. Ding, *Scattering of Electromagnetic Waves, Vol. 1: Theory and Applications*, Wiley Interscience, 2000.

[16] P. Dubois-Fernandez, J.-C. Souyris, S. Angelliaume, F. Garestier, "Compact polarimetry at low frequency", *IEEE Trans. Geosci. Remote Sens.*, vol. 46, no. 10, pp. 3208–3221, Oct. 2008

[17] S. R. Cloude and E. Pottier, "An entropy based classification scheme for land applications of polarimetric SAR," *IEEE Trans. Geosci. Remote Sens.*, vol 35, no. 1, pp. 68-78, Jan. 1997.

[18] J.S. Lee , and E. Pottier, *Polarimetric radar imaging: from basics to application*, CRC Press, Taylor & Francis Group, Boca Raton, 2009.

[19] K. Raney, J. T.S. Cahil, G. W. Patterson and D.B.J. Bussey, "The M-Chi decomposition of hybrid dual-polarimetric radar data," *Proc. of IGARSS-11*, 22-27 July 2011, Munich, Germany, 2012.

[20] S.R. Cloude, D.G. Goodenough, and H. Chen, "Compact decomposition theory," *IEEE Geosci. Remote Sens.Lett.*, vol. 9, no. 1, pp. 28-32, Jan. 2012.

[21] G. Singh, Y. Yamaguchi, G. Venkataraman and S.-E. Park, "General four component scattering power decomposition with unitary transformation of coherency matrix," *IEEE Trans. Geosci. Remote Sens.* vol. 51, no.5, pp. 3014-3022, May 2013.

[22] Y. Yamaguchi, A. Sato, W.-M. Boerner, R. Sato, and H. Yamada, "Four-component scattering power decomposition with rotation of coherency matrix," *IEEE Trans. Geosci. Remote Sens.*, vol. 49, no. 6, pp. 2251 – 2258, 2011.

[23] G. Singh, Y. Yamaguchi, G. Venkataraman and S.-E. Park, "Potential assessment of SAR in compact and full polarimetry mode for snow detection", *Proc. of IGARSS-11*, 24-30 July 2011, Vancouver, Canada, 2011.

[24] J. S. Lee, M. R. Grunes, E. Pottier, "Quantitative comparison of classification capability: Fully polarimetric versus dual-and single-polarization SAR. *IEEE Trans. Geosci. Remote Sens.*, vol. 39, no. 11, pp. 2343-2351, 2001.

[25] Q. McNemar, "Note on the sampling error of the difference between correlated proportions or percentages", *Psychometrika* , vol. 12, no. 2, pp. 153–157, 1947.

[26] J De Leeuw, H. Jia, L. Yang, X. Liu, K. Schmidt, and A.K. Skidmore, "Comparing accuracy assessments to infer superiority of image classification methods", *Int. J. Remote Sens.* Vol. 27, no.1, pp. 223–232, 2006.

Gulab Singh (S'9–SM'10) was born in Salooni-Sarsawa-Saharanpur, Uttar Pradesh, India, in 1976. He received the B.Sc. and M.Sc. degrees in physics from the Chaudhary Charan Singh University (formerly Meerut University), Meerut, India, in 1998 and 2000, respectively, the M.Tech. degree in remote sensing from the Birla Institute of Technology, Ranchi, India, in 2005, the Ph.D. degree from the Indian Institute of Technology Bombay, Mumbai, India, in 2011, and Dr. Eng. in Electrical and Information Engineering from the Niigata University, Niigata, Japan, in 2013.

From 2002 to 2003, he was a Physics Lecturer at Janata (public) Inter College Jhabiran, Saharanpur, Uttar Pradesh, India. From 2005 to 2007, he was a Senior Research Fellow at the Centre of Studies in Resources Engineering, Indian Institute of Technology Bombay, where he was involved in several research projects related to POLSAR and InSAR data analysis for snow and ice parameters retrieval. Since April 2010, he has been a Postdoctoral Fellow at the Graduate School of Science and Technology, Niigata University, Niigata, Japan. His current research interests include SAR data analysis, SAR polarimetry, and SAR interferometry techniques development for Earth and lunar surface parameters estimation.

Dr. Singh was honored with the ''Award for Excellence in Thesis Work'' for his outstanding research contributions from the Indian Institute of Technology Bombay on August 5, 2011.

Yoshio Yamaguchi (M'83–SM'94-F'02) received the B.E. degree in electronics engineering from Niigata University, Niigata, Japan, in 1976 and the M.E. and Dr. Eng. degrees from Tokyo Institute of Technology, Tokyo, Japan, in 1978 and 1983,respectively. In 1978, he joined the Faculty of Engineering, Niigata University. From 1988 to 1989, he was a Research Associate at the University of Illinois at Chicago, Chicago. He is currently with the Graduate School of Science and Technology, Niigata University. His interests are in the field of radar polarimetry, microwave sensing, and imaging.

Dr. Yamaguchi is a Fellow of the Institute of Electronics, Information and Communication Engineers, Japan. He has also served as Chair of the IEEE Geoscience and Remote Sensing Society (GRSS) Japan Chapter (2002–2003), Chair of the International Union of Radio Science Commission F Japanese Committee (URSI-F) Japan (2006–2011), Associate Editor for Asian Affairs of the GRSS Newsletter (2003–2007), and Technical Program Committee Cochair of the 2011 IEEE International Geoscience and Remote Sensing Symposium.

He was a recipient of the 2008 IEEE GRSS Education Award.

Sang-Eun Park (S'05–M'07) received the B.S. and M.S. degrees in geophysics and the Ph.D. degree in radar remote sensing and geophysics from Seoul National University, Seoul, Korea, in 2000, 2002, and 2007, respectively.

From 2007 to September 2009, he was with the Radar Polarimetry Remote Sensing Group of the University of Rennes 1, Rennes, France, for a postdoctoral fellowship on radar polarimetry. From October 2009 to January 2010, he was a Project Scientist in the Institute of Photogrammetry and Remote Sensing, Vienna University of Technology, Vienna, Austria. He is currently an Assistant Professor in the Graduate School of Science and Technology, Niigata University, Niigata, Japan. His research interests include polarimetric SAR classification, forward and inverse modeling of microwave vegetation and surface backscattering, and investigation of multisource data integration methodology.

Wolfgang-Martin Boerner (SM'75–F'84–LF'92) received the Ph.D. degree from the University of Pennsylvania, Philadelphia, in 1967. From 1967 to 1968, he was with the University of Michigan, Ann Arbor. In 1968, he was with the University of Manitoba, Winnipeg, MB, Canada. Since 1978, he has been a Professor with the Department of Electrical and Computer Engineering, University of Illinois at Chicago, Chicago. His research interests include electromagnetic vector inverse scattering, radar polarimetry, polarimetric interferometry, and tomography.

Dr. Boerner is a member of numerous international scientific societies. He is a Senior Member of CAP, American Society for Engineering Education, ASRSP, and ISRSP and a Fellow of the Optical Society of America, International Society for Optics and Photonics (SPIE), American Association for the Advancement of Science, The Institute of Electronics, Information and Communication Engineers. He is a member of the honor societies Sigma Xi, the American and German Fulbright Associations, and the Alexander von Humboldt Association.

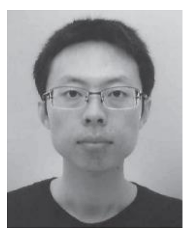

Yi Cui (S'09–M'11) received the B.S. degree (with honors) in electronic information science and technology from Jilin University, Changchun, China, in 2006 and the Ph.D. degree in information and communication engineering from the Tsinghua University, Beijing, China, in 2011.

He is currently a Postdoctoral Research Fellow with Niigata University, Niigata, Japan. His research interests include signal and image processing and their applications in SAR remote sensing, radar polarimetry, and electromagnetic theory.

Dr. Cui is the first-prize winner of the student paper competition at the 2010 Asia-Pacific Radio Science Conference in Toyama, Japan.

Gopalan Venkataraman received the M.Sc. and Ph.D. degrees in applied geology from the Indian Institute of Technology Bombay, Mumbai, India, in 1971 and 1976, respectively. He has been with the Centre of Studies in Resources Engineering, Indian Institute of Technology Bombay, India since 1976. He has been carrying out research in remote sensing and GIS applications to geological and environmental problems. He visited ITC (Enschede and Delft), The Netherlands, on a scientific exchange program for research in the area of Spatial modeling for mineral experience in 1989. He has also carried out many research projects in the field of remote sensing applications to the mineral exploration, environmental impact of mining and desertification for ISRO, DST, Ministry of Environmental and Forest. For the last 20 years, he has been emphasizing on research relating to snow and glaciers studies particularly involving active and passive microwave remote sensing data.